

DISKS SURVIVING THE RADIATION PRESSURE OF RADIO PULSARS

K. YAVUZ EKŞİ¹ AND M. ALİ ALPAR

Sabancı University, 34956, Orhanlı-Tuzla, İstanbul, Turkey
(Received 2004 July 2; Accepted 2004 Sep 13)
Draft version November 26, 2018

ABSTRACT

The radiation pressure of a radio pulsar does not necessarily disrupt a surrounding disk. The position of the inner radius of a thin disk around a neutron star, determined by the balance of stresses, can be estimated by comparing the electromagnetic energy density generated by the neutron star as a rotating magnetic dipole in vacuum with the kinetic energy density of the disk. Inside the light cylinder, the near zone electromagnetic field is essentially the dipole magnetic field, and the inner radius is the conventional Alfvén radius. Far outside the light cylinder, in the radiation zone, $|\mathbf{E}| = |\mathbf{B}|$ and the electromagnetic energy density is $\langle S \rangle / c \propto 1/r^2$ where \mathbf{S} is the Poynting vector. Shvartsman (1970) argued that a stable equilibrium can not be found in the radiative zone because the electromagnetic energy density dominates over the kinetic energy density, with the relative strength of the electromagnetic stresses increasing with radius. In order to check whether this is true also near the light cylinder, we employ global electromagnetic field solutions for rotating oblique magnetic dipoles (Deutsch 1955). Near the light cylinder the electromagnetic energy density increases steeply enough with decreasing r to balance the kinetic energy density at a stable equilibrium. The transition from the near zone to the radiation zone is broad. The radiation pressure of the pulsar can not disrupt the disk for values of the inner radius up to about twice the light cylinder radius if the rotation axis and the magnetic axis are orthogonal. This allowed range beyond the light cylinder extends much further for small inclination angles. The mass flow rate in quiescent phases of accretion driven millisecond pulsars can occasionally drop to values low enough that the inner radius of the disk goes beyond the light cylinder. The possibilities considered here may be relevant for the evolution of spun-up X-ray binaries into millisecond pulsars, for some transients, and for the evolution of young neutron stars if there is a fallback disk surrounding the neutron star.

Subject headings: accretion disks— stars: individual SAX J1808.4–3658, Aquila X–1—stars: neutron—X-rays: binaries

1. INTRODUCTION

A neutron star can interact with a surrounding disk in a variety of modes. These different modes of interaction can lead to various astrophysical manifestations and are of key importance in classifying neutron stars. The mode of interaction and hence the evolutionary stage is determined by the location of the inner radius of the disk with respect to the characteristic radii, the corotation radius $R_c = (GM/\Omega^2)^{1/3}$ and the light cylinder radius $R_L = c/\Omega$ where Ω is the angular velocity and M is the mass of the neutron star. Starting with the pioneering work of Shvartsman (1970a), three basic modes of interaction—accretor, propeller and ejector—(Lipunov 1992) of a neutron star with a surrounding disk have been identified. If the inner radius of the disk is beyond the corotation radius, the system is expected to be in the propeller stage (Shvartsman 1970a; Illarionov & Sunyaev 1975; Davidson & Ostriker 1973; Fabian 1975). The ejector (radio pulsar) stage is assumed to commence when inner radius is also beyond the light cylinder radius.

The disk should be disrupted in the region where magnetic and matter stresses are comparable (Pringle & Rees 1972; Davidson & Ostriker 1973; Lamb, Pethick & Pines 1973) and the inner radius of the disk, R_{in} , is estimated by balancing the kinetic energy density (half the ram pressure) of the disk with the electromagnetic energy density (same as electromagnetic pressure) of the radiation generated by the neutron star. In or-

der that the equilibrium found in this way is stable, the electromagnetic energy density at $r < R_{in}$ should be greater than the kinetic energy density, i.e. the electromagnetic energy density at R_{in} should increase more steeply than the kinetic energy density in approaching the star (Lipunov 1992). The usual estimate for the kinetic energy density has the dependence $\mathcal{E}_K \propto r^{-5/2}$ (see §3) on the radial distance r from the center of the neutron star. In the near zone ($R_* < r \ll R_L$) where R_* is the radius of the neutron star, electric energy density, \mathcal{E}_e , is negligible and the kinetic energy density is balanced essentially by the magnetic energy density, \mathcal{E}_m , of the dipole field of the neutron star at the Alfvén radius. This is a stable equilibrium point because $\mathcal{E}_{em} \propto r^{-6}$ is steep enough to balance $\mathcal{E}_K \propto r^{-5/2}$ i.e. $\mathcal{E}_{em} > \mathcal{E}_K$ for $r < R_{in}$ and $\mathcal{E}_K > \mathcal{E}_{em}$ for $r > R_{in}$. In the radiation zone ($r \gg R_L$) where electromagnetic energy density $\mathcal{E}_{em} \propto r^{-2}$, a stable inner boundary can not be found because then \mathcal{E}_K would be greater than \mathcal{E}_{em} for $r < R_{in}$ and $\mathcal{E}_{em} > \mathcal{E}_K$ for $r > R_{in}$, and the disk is disrupted. This was first noticed by Shvartsman (1970b) who with the above argument concluded that the stable equilibrium outside the light cylinder would only be possible beyond the gravitational capture radius (Lipunov 1992).

Usual estimates employ a rotating magnetic dipole in vacuum to generate the electromagnetic fields of the neutron star. In the near zone ($R_* < r \ll R_L$) the magnetostatic energy density $B^2/8\pi$ is employed, while in the radiation zone ($r \gg R_L$), at distances far outside the light cylinder, the radiation pressure $\langle S \rangle / c$, where \mathbf{S} is the Poynting vector, is used. For simplicity one usually employs a piecewise defined electromagnetic energy density which scales as r^{-6} for $r < R_L$ and as r^{-2}

¹ Present address: Harvard-Smithsonian Center for Astrophysics, 60 Garden Street, Cambridge, MA 02138; yeksi@cfa.harvard.edu
Electronic address: yavuz@sabanciuniv.edu, alpar@sabanciuniv.edu

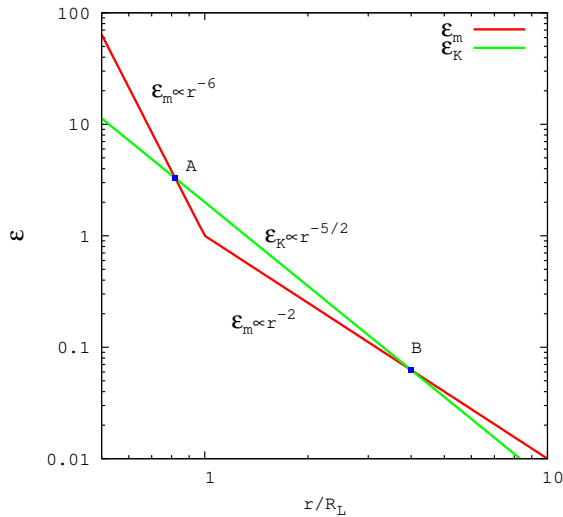


FIG. 1.— Two possible equilibrium configurations around a rotating dipole. Equilibrium at the near zone (point A = Alfvén radius) is stable because magnetic energy density drops more rapidly than the kinetic energy density going beyond this point. Equilibrium at the radiation zone (point B) is not stable because the magnetic pressure drops less rapidly than kinetic energy density and disrupts the disk beyond this point. With a piecewise defined field configuration as above, one has to conclude that the disk has to be disrupted once the inner radius goes beyond R_L . (This figure is not included in the accepted paper. It is added for explanatory purposes.)

for $r > R_L$. With such a model one necessarily concludes that the disk will be disrupted if the inner radius of the disk goes beyond the light cylinder radius (see Figure 1).

In this work we present the full expressions for electromagnetic pressure around a rotating dipole in vacuum, reducing to the conventional expressions in the near zone and the radiation zone, and describing the transition across the light cylinder. We use these results to investigate the location and stability of the Alfvén radius and inner radius of thin Keplerian disks. This information is relevant if the mass flow rate through the disk declines or the neutron star rotation period evolves such that the inner radius is beyond the light cylinder. According to the conventional pulsar magnetosphere models (Goldreich & Julian 1969), the pulsar activity can commence if the inner radius is outside the light cylinder. According to the simple piecewise model described above, the disk would be swept away. In the present model with a rather broad transition from the near zone to the radiation zone, there will be a wide range of allowed values for the mass flow rate for which the inner radius of the disk is outside the light cylinder while the disk can survive the radiation pressure. In this case, the pulsar activity will commence but depending on the inclination angle, the presence of the disk may destroy the coherent pulsed emission in the radio band.

In its quiescent stage, the luminosity of the accretion driven millisecond pulsar SAX J1808.4-3658 (Wijnands & van der Klis 1998) drops below $L_x \sim 10^{32}$ erg s $^{-1}$ (Campana et al. 2002). Assuming the system passes through a propeller stage the mass inflow rate, which determines the inner radius, can be much greater than the mass accretion rate on to the star determining the luminosity. As we do not know what fraction of the inflowing mass can accrete in the propeller stage, we can not estimate the inner radius from the observed luminosity. Assuming 1 per cent of the inflowing mass accretes on to the star, we would estimate an inner radius for the disk greater than the light cylinder.

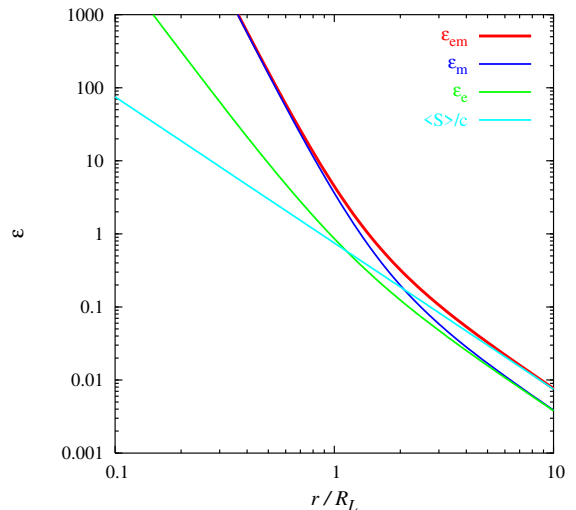


FIG. 2.— Radial structure of the electromagnetic energy density around the pulsar. *Solid* (colored red in electronic edition) line is the electromagnetic energy density, *long dashed* (colored green in electronic edition) line is the electrical energy density $E^2/8\pi$, *short dashed* (colored dark blue in electronic edition) line is the magnetic energy density $B^2/8\pi$, and *dashed and dotted* (colored light blue in electronic edition) line is $\langle S_r \rangle / c$. Magnetic energy density dominates inside the light cylinder radius. Far outside the light cylinder electric and magnetic energy densities become equal and $\langle S_r \rangle / c$ is equal to their sum. See the electronic edition of the Journal for a color version of this figure.

Burderi et al. (2003) suggested that the optical properties of this source in the quiescent stage indicate an active pulsar (see also Campana et al. (2004)). We find that such a disk can survive the radiation pressure of a turned on rotation-powered pulsar. This may be the case in some stages of transients (e.g. Campana et al. (1998); Zamanov (1995)) and of the evolution of young neutron stars if they have fallback disks (Michel & Dessler 1981; Marsden et al. 2001b, 2002; Menou et al. 2001; Alpar et al. 2001; Ekşi & Alpar 2003).

In §2 we derive the electromagnetic energy density from the global electromagnetic field solution of Deutsch (1955) for obliquely rotating magnetic dipoles. In §3 we derive the inner radius of the disk. In §4 we discuss implications for the accretion driven millisecond pulsar SAX J1808.4-3658 which is probably representative of the millisecond X-ray pulsars, for certain other transients and for fallback disks around radio pulsars. In §5 we discuss our results.

2. ELECTROMAGNETIC ENERGY DENSITY

A rotating dipole can radiate electromagnetic energy if the spin and magnetic axes are not aligned. A global solution for a perfectly conducting, rigidly rotating star in vacuum was first given by Deutsch (1955). The relevance of this solution for radio pulsars is thoroughly discussed by Michel & Li (1999).

The early papers on pulsars (Ostriker & Gunn 1968; Pacini 1967, 1968; Michel & Goldwire 1970; Davis & Goldstein 1970) employed the vacuum solutions of Deutsch (1955). The vacuum assumption can not actually be realized for neutron stars because the magnetospheric field itself is strong enough to tear off electrons from the surface of the neutron star. Indeed, Goldreich & Julian (1969) showed that an axisymmetric pulsar magnetosphere should have a corotating plasma described by the hydromagnetic approximation $\mathbf{E} + \mathbf{v} \times \mathbf{B} = 0$ with a corresponding charge density $\nabla \cdot \mathbf{E}$. Whether the pulsar electrodynamics is dominated by the

Goldreich & Julian (1969) currents, or by the vacuum fields modified by rather smaller currents is still of debate (Michel 1991) and a global self-consistent solution of the problem is yet to be presented. Kaburaki (1981) argued that the existence of a corotating plasma does not alter the field structure drastically because it simply means an effective increase in the radius of the conducting star (see Melatos (1997) for an application of this idea) using the Deutsch (1955) solution. The presence of the disk might alter the field structure (e.g. Elsner & Lamb (1977)) even more than the corotating plasma and further complicate the magnetospheric currents (Treves & Szuszkiewics 1995). In the absence of a consistent solution of the problem of the pulsar magnetosphere with corotating plasma with or without a disk, we, for simplicity, employ the Deutsch (1955) solutions for a rotating dipole in vacuum. We quote the field solutions of Deutsch (1955), as corrected by Michel & Li (1999), in the Appendix, and use them in our estimation of the electromagnetic energy density at the disk plane. As Maxwell's equations do not preserve their form in rotating coordinates the problem of rotating dipoles is intrinsically relativistic. These solutions can be shown to be the limiting case for slow rotation (see e.g. Belinski et al. (1994)).

As obtained in the Appendix, the radial component of the Poynting vector $\mathbf{S} = (c/4\pi)\mathbf{E} \times \mathbf{B}$ at the disk plane (zenith angle $\theta = \pi/2$) averaged over a stellar period is

$$\frac{\langle S_r \rangle}{c} = \frac{\mu^2}{8\pi R_L^6} \frac{\sin^2 \xi}{x^2} \quad (1)$$

Here ξ is the angle between the magnetic moment μ and the rotation rate Ω of the neutron star, and $x = r/R_L$. Note that Eq. (1) is accurate only for $\alpha = R_*/R_L \ll 1$. For the fastest millisecond pulsar with $P \cong 1.5$ ms, $\alpha = 0.14$, thus $\alpha \ll 1$ holds for pulsars; in this case $\langle S_r \rangle/c \propto r^{-2}$ for r greater than a few R_* , (see Eqs. (A13)-(A15)).

The dynamical disk time-scale is much longer than the period of the neutron star. The disk would only “see” the average field of many stellar rotations. We average the squared fields over one stellar period P as $\langle B_i^2 \rangle = (1/P) \int_0^P B_i^2 dt$ where B_i is any component of the magnetic field, and obtain the magnetic energy density $\mathcal{E}_m = \langle B^2 \rangle / 8\pi$ as (see Appendix)

$$\mathcal{E}_m \simeq \frac{\mu^2}{8\pi R_L^6} x^{-6} \left[\cos^2 \xi + \frac{1}{2} (x^4 + 3x^2 + 5) \sin^2 \xi \right] \quad (2)$$

for $\alpha \ll 1$.

Similarly, in the $\alpha \ll 1$ approximation, the electric energy density $\mathcal{E}_e = \langle E^2 \rangle / 8\pi$ is (see Appendix)

$$\mathcal{E}_e \simeq \frac{\mu^2}{8\pi R_L^6} x^{-4} \left[\frac{4}{9} \cos^2 \xi + \frac{1}{2} (x^2 + 1) \sin^2 \xi \right] \quad (3)$$

The total electromagnetic energy density can be found by summing up the magnetic and electric energy densities. From equations (2) and (3), one finds

$$\mathcal{E}_{em} = \frac{\mu^2}{8\pi R_L^6} x^{-6} \left[\left(1 + \frac{4}{9} x^2 \right) \cos^2 \xi + \left(x^4 + 2x^2 + \frac{5}{2} \right) \sin^2 \xi \right] \quad (4)$$

Note that this reduces to $\mathcal{E}_{em} \propto r^{-6}$ for $r \ll R_L$ and $\mathcal{E}_{em} \propto r^{-2}$ for $r \gg R_L$, as expected. We show \mathcal{E}_{em} together with \mathcal{E}_m , \mathcal{E}_e , and $\langle S_r/c \rangle$, all scaled with $\mu^2/8\pi R_L^6$, in Figure (2). If the sole effect of the corotating plasma is to increase the radius of the region beyond which vacuum starts from R_* to a larger value

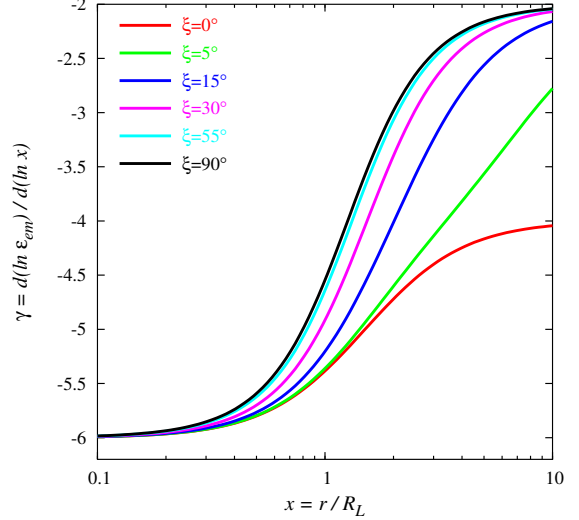


FIG. 3.— Power-law index of the electromagnetic energy density for a variety of inclination angles. The power-law index changes between -6 and -2. The transition becomes broader for small inclination angles. See the electronic edition of the Journal for a color version of this figure.

R_v (Melatos 1997), then $\alpha \equiv R_v/R_L$ can have values close to unity. In this case the expression for the total energy density is more complex than equation (4), the coefficients having terms with powers of α . The behavior of \mathcal{E}_{em} and its constituents do not change qualitatively for $\alpha \lesssim 1$ if we retain such terms.

The local power-law index of electromagnetic energy density, $\gamma \equiv d \ln \mathcal{E}_{em} / d \ln x$, calculated from equation (4) is

$$\gamma = -6 + \frac{(8/9)x^2 \cos^2 \xi + 4x^2 (x^2 + 1) \sin^2 \xi}{[1 + (4/9)x^2] \cos^2 \xi + (x^4 + 2x^2 + 5/2) \sin^2 \xi} \quad (5)$$

We show γ for a variety of ξ in Figure (3).

The value of γ at the light cylinder, $\gamma_L \equiv \gamma(x=1)$, from equation (5), is

$$\gamma_L = -6 + \frac{(8/9) \cos^2 \xi + 8 \sin^2 \xi}{(13/9) \cos^2 \xi + (11/2) \sin^2 \xi} \quad (6)$$

and is plotted in Figure (4). The kinetic energy density scales with $x^{-5/2}$ (see the following section). Note that for all inclination angles $\gamma_L < -5/2$ i.e. the electromagnetic energy density is steep enough to balance the kinetic energy density of the disk at the light cylinder.

The radius beyond which $\gamma > -5/2$ can be found by solving equation (5) for $\gamma = -5/2$. We find this to be

$$x_{crit} = \frac{\sqrt{6}}{6 \tan \xi} \sqrt{4 + 18 \tan^2 \xi + \sqrt{16 + 396 \tan^2 \xi + 954 \tan^4 \xi}} \quad (7)$$

Figure 5 shows that the disk inner radius will be stable beyond the light cylinder, for distances up to many R_L , practically for all radii for aligned ($\xi = 0^\circ$) rotators and up to $r_{crit} \cong 3R_L$ for orthogonal ($\xi = 90^\circ$) rotators.

3. THE INNER RADIUS NEAR THE LIGHT CYLINDER

We estimate the inner radius as the electromagnetic radius R_{em} , determined by $\mathcal{E}_{em} = \mathcal{E}_K$ taking the conventional estimate $\mathcal{E}_K = \frac{1}{2} \rho |\mathbf{v}| v_{ff}$ where $\rho |\mathbf{v}| = \dot{M} / 4\pi r^2$ is from the conservation of mass in spherical coordinates, \dot{M} being the mass flow rate,

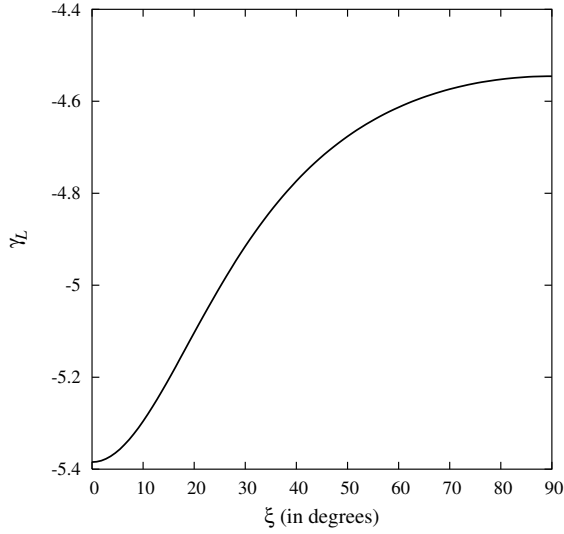


FIG. 4.— Power-law index of the electromagnetic energy density at the light cylinder ($x = 1$), changing with the inclination angle.

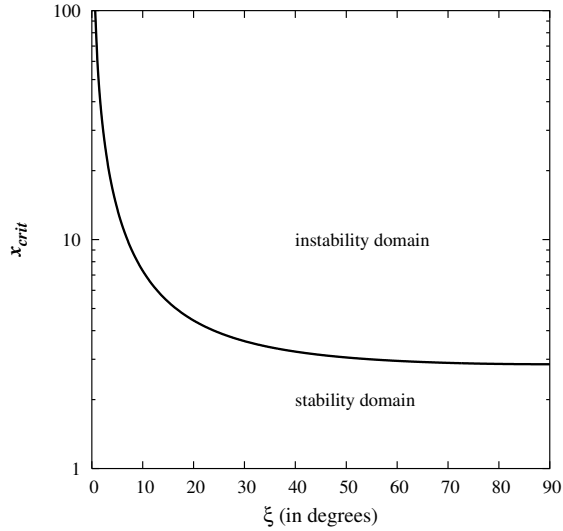


FIG. 5.— The critical radius, in terms of light cylinder radius at which $\gamma = -5/2$, as given in equation (7).

and $v_{ff} = \sqrt{2GM/r}$ is the free-fall velocity. This gives

$$\mathcal{E}_K = \frac{\dot{M} \sqrt{2GM}}{8\pi R_L^{5/2}} x^{-5/2}. \quad (8)$$

The electromagnetic radius can be found using equations (4) and (8):

$$x_{em}^{7/2} = x_A^{7/2} \left[\left(1 + \frac{4}{9} x_{em}^2\right) \cos^2 \xi + \left(x_{em}^4 + 2x_{em}^2 + \frac{5}{2}\right) \sin^2 \xi \right]. \quad (9)$$

Here $x_A = R_A/R_L$ and

$$R_A = \left(\frac{\mu^2}{\dot{M} \sqrt{2GM}} \right)^{2/7} \quad (10)$$

is the Alfvén radius.

The solution of equation (9) for $x_{em}(x_A)$ is given in Figure (6) for a variety of ξ . It is not possible to find a solution for every x_A , corresponding to the fact that at low mass transfer rates, the kinetic energy density of the disk can not match

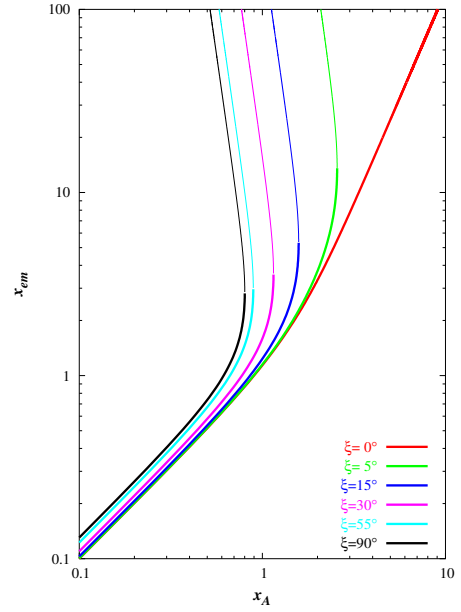


FIG. 6.— The variation of x_{em} with x_A as determined from Eq. (9), for a variety of inclination angles. See the electronic edition of the Journal for a color version of this figure.

the electromagnetic energy density at any radius, and the disk will be ejected. The lowest mass flow rate for which the disk will not be ejected corresponds to the maximum $x_A(x_{em})$ as seen in Figure (6). From $dx_A/dx_{em} = 0$ follows the solution (7) as expected. Now using this back in equation (9) one finds the critical Alfvén radius

$$x_{A,crit} = x_{crit} \left[\left(1 + \frac{4}{9} x_{crit}^2\right) \cos^2 \xi + \left(x_{crit}^4 + 2x_{crit}^2 + \frac{5}{2}\right) \sin^2 \xi \right]^{-2/7} \quad (11)$$

corresponding to the single solution $x_{em} = x_{crit}$ and to the critical mass flow rate

$$\dot{M}_{crit} = \frac{\mu^2}{\sqrt{2GM} R_L^{7/2} x_{A,crit}^{-7/2}}. \quad (12)$$

For higher mass flow rates there will be two solutions for x_{em} the smaller of which is the stable one. This stable solution is beyond the light cylinder for a range of mass flow rates $\dot{M}_{crit} < \dot{M} < \dot{M}_L$ where \dot{M}_L is the flow rate for which the inner radius will be at the light cylinder, $x_{em} = 1$. This will happen when x_A attains the value

$$x_{A,L} = \left(\frac{13}{9} \cos^2 \xi + \frac{11}{2} \sin^2 \xi \right)^{-2/7} \quad (13)$$

as can be obtained from equation (9). Hence

$$\dot{M}_L = \frac{\mu^2}{\sqrt{2GM} R_L^{7/2} x_{A,L}^{-7/2}} \quad (14)$$

is obtained. Note that both \dot{M}_{crit} and \dot{M}_L are strongly dependent on the period and the magnetic moment of the neutron star ($\dot{M}_L \propto \dot{M}_{crit} \propto P^{-7/2} \mu^2$) and their ratio is only dependent on the inclination angle ξ . The range of mass flow rates and inner disk radii for which the disk is beyond the light cylinder, and stable, is smallest for $\xi = 90^\circ$; for which $R_{crit} \cong 3R_L$ and $\dot{M}_{crit} = 0.4\dot{M}_L$.

Within the model the disk will survive beyond the light cylinder, even if the radio pulsar activity turns on. As long

as \dot{M} remains larger than \dot{M}_{crit} (i.e. $R_A < R_{A,crit}$), the disk will not be ejected, and the radio pulsar may turn off again when \dot{M} increases to \dot{M}_L , switching back to the propeller phase. The threshold for quenching the radio pulsar will reflect loading of all closed field lines that lead to the inner gap with plasma from the disk. This does not necessarily happen at $R_{em} = R_L$. If the transition to radio pulsar activity happens at some radius $R_r(\xi) < R_L$, then the transient radio pulsar phase with the disk not ejected prevails for $\dot{M} < \dot{M}_r$, corresponding to $R_{em} > R_r$.

The scaling we have used which reduces to the Alfvén radius for $r \ll R_L$ presumes a spherical accretion flow. The Shakura & Sunyaev (1973) solutions for thin Keplerian disks asymptotically imply that the density of the gas in the disk scales as $\rho \propto r^{-15/8}$. Hence $\mathcal{E}_K \propto \rho v_K^2 \propto \rho r^{-1} \propto r^{-23/8}$. This scaling ($\gamma = -23/8 = -2.875$) is slightly more steep than what we have used $\gamma = -5/2$. For a Shakura-Sunyaev thin disk, our estimate for the critical inner radius will be somewhat smaller than the estimate given above. From Eq. (7) the minimum critical radius ($\xi = 90^\circ$) is $x_{crit,min} = 2.85$ while for $\gamma = -2.875$ we would obtain $x_{crit,min} = 2.13$.

4. APPLICATIONS

4.1. SAX J1808.4-3658, Other Millisecond X-ray Pulsars and Transients

The rotation periods of accretion driven millisecond pulsars (Wijnands 2004) range between 2.3 ms to 5.4 ms. We take the first discovered (Wijnands & van der Klis 1998) accretion driven millisecond pulsar SAX J1808.4-3658 with a rotation period $P = 2.5$ ms as an example of this class. The upper limit on the magnetic field of the neutron star is 5×10^8 Gauss (Di Salvo & Burderi 2003). We assume the magnetic moment to be $\mu = 3 \times 10^{26}$ Gauss cm³. Using these parameters in equations (12) and (14) we obtain the results shown in Figure 7 for SAX J1808.4-3658. For mass flow rates greater than 10^{13} g s⁻¹ for an inclination angle $\xi = 10^\circ$ and greater than 2×10^{14} g s⁻¹ for an inclination angle $\xi = 90^\circ$, the source can sustain a disk beyond the light cylinder and thus can be in a rotation powered pulsar phase. The region between the two curves represents the mass inflow rate for which the electromagnetic radius is larger than the light cylinder while the disk can survive the pulsar activity. At mass inflow rates \dot{M}_L greater than a few 10^{14} g s⁻¹ for all inclination angles, the disk inner radius will protrude into the light cylinder, and magnetospheric pulsar activity will be quenched by the presence of the disk to the extent that all field lines are loaded with plasma from the disk. The source will probably be in a propeller phase with only a fraction of the mass inflow possibly being accreted while the rest is diverted into an outflow. When the inner radius of the disk is of the order of the corotation radius, accretion of the full mass flow rate is expected. We estimate mass inflow rates of the order of 10^{16} g s⁻¹ for this transition for all inclination angles. The maximum luminosity of SAX J1808.4-3658 in outburst is $\sim 2 \times 10^{35}$ erg s⁻¹, which corresponds to a mass accretion rate of 10^{14} g s⁻¹. The discrepancy is probably related to our scaling of the disk inner radius with the Alfvén radius, and the uncertainties in the determination of the Alfvén radius as well as to the simplifications of the present model in terms of the vacuum dipole solutions. In quiescence the luminosity drops to $\sim 10^{32}$ erg s⁻¹ (Campana et al. 2002). It is possible that the mass inflow rate in the disk is large enough that the inner radius of the disk is inside the light cylinder but only a very small fraction ($\lesssim 0.1$ percent) of this inflowing mass accretes onto the neutron star, producing the observed X-ray

luminosity. Burderi et al. (2003) argued that the irradiation of the companion by the switched on magneto-dipole rotator, in the quiescent stage, can explain the modulation of the flux in the optical (see also Campana et al. (2004)). If the source is in the propeller stage accretion of only a small fraction of the disk inflow through a limited bunch of field lines will probably allow the magnetospheric gaps and pulsar radiation to survive. This would be easier for the outer gaps. Magnetospheric voltages in millisecond pulsars are of the order of those in the Vela pulsar, so optical, X and gamma ray pulsar activity may be possible if the outer gap can survive. For small inclination angles accretion near the magnetic polar caps would also be near the rotational pole and therefore avoiding the centrifugal barrier. For paths avoiding the inner gap even radio pulsar activity might survive in the propeller phase, with the disk protruding inside the light cylinder. Depending on the beaming geometry searches for radio and high energy pulsar activity might yield very interesting results. SAX J1808.4-3658 was selected for this discussion as it is the millisecond X-ray pulsar with the most detailed information (Wijnands 2004). This discussion applies to the other millisecond X-ray pulsars also.

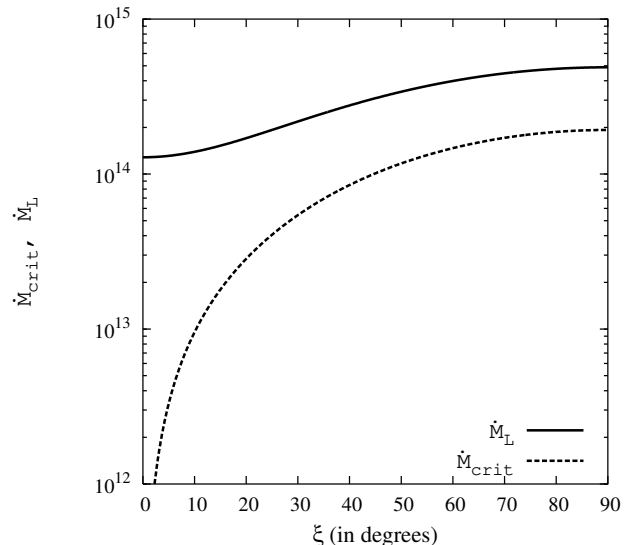


FIG. 7.— The mass flow rate range for SAX J1808.4–3658 for which the inner radius is outside the light cylinder while the disk is not swept away by the radiation pressure. The solid line corresponds to \dot{M}_L (eqn. 14) and the dashed line corresponds to \dot{M}_{crit} (eqn. 12). The domain between the curves corresponds to the allowed mass flow range for which the inner radius is outside the light cylinder while the disk is not disrupted. The observed luminosity may be much lower than that would correspond to these mass flow rates because the centrifugal barrier will not allow all inflowing mass to accrete onto the neutron star. For small inclination angles the allowed mass flow rate range increases.

Other transient low mass X-ray binaries (LMXBs) may also be in phases that include excursions of the inner disk towards and beyond the light cylinder and back. As an example, the luminosity of Soft X-ray Transient Aquila X-1 was observed Campana et al. (1998) to decay from $\sim 10^{36}$ erg s⁻¹ to $\sim 10^{33}$ erg s⁻¹, from outburst to the quiescent stage. As the system in the quiescent stage is likely to be in the propeller mode, the observed luminosity of $\sim 10^{33}$ erg s⁻¹ reflects a small fraction of the inflowing mass that accretes. The present discussion adds to the possibilities that of occasional rotation powered pulsar activity. The uncertainty in rotation period and magnetic field does not allow a more detailed discussion in terms of our model. Further, the majority of LMXBs do not exhibit

rotation periods in their accretion and propeller phases for reasons of selection in the source, and this is probably also the case for most transients.

4.2. Implications for Fallback Disks

Neutron stars are born in supernova explosions. It is a possibility that some of the ejected matter fails to achieve the escape velocity and falls back (Woosley, Heger & Weaver 2002). As the progenitor is rotating, the fallback matter might have enough angular momentum to settle into a disk (Mineshige et al. 1997). The idea of fallback disks around pulsars dates back to Michel & Dessler (1981). The fallback disk model (Chatterjee et al. 2000; Alpar 2001; Marsden et al. 2001a; Ekşi & Alpar 2003) of anomalous X-ray pulsars (Mereghetti et al. 2002; Kaspi 2004) renewed interest in possible implications for radio pulsars (Michel & Dessler 1981; Marsden et al. 2001b, 2002; Menou et al. 2001; Alpar et al. 2001). More recently Blackman & Perna (2004) suggested that the observed jets of Crab and Vela may be collimated by fallback disks.

Young neutron stars might follow a variety of evolutionary paths depending on the initial mass of their fallback disks (Alpar 2001). The evolutionary stages are determined by the mode of interaction discussed in §1. As the mass of a fallback disk is not replenished, mass flow rate in the disk declines and the inner radius of the disk, as a consequence, moves out. As the neutron star is initially spinning down with propeller torques, the light cylinder is also moving out, though less rapidly than the inner radius. At some stage the inner radius will catch up with the light cylinder.

Menou et al. (2001) and Alpar et al. (2001) assumed that the inner radius of fallback disks tracks the light cylinder radius. In such a model the disk can assist the magnetic dipole radiation torque without quenching the radio pulsar mechanism. These models would not work (Li 2002) if the disruption of the disk takes place (Shvartsman 1970b) as soon as its inner edge reaches the light cylinder from within the near zone. The present work shows that such a disk need not be necessarily disrupted till its inner radius moves to a few times the light cylinder radius. Whether the inner radius can actually track the light cylinder for a long epoch, rather than moving beyond the light cylinder into the radiation zone, will be studied in a subsequent paper.

5. CONCLUSION

We have shown that the electromagnetic energy density of a rotating dipole makes a rather broad transition across the light cylinder from the near zone dipole magnetic field to the

radiation zone, the transition being broader for small inclination angles, ξ . For power-law indices γ for the r dependence of the electromagnetic energy density, $\gamma > -5/2$, the regime in which the radiation pressure would eject the disk, is not attained until r exceeds a few R_L depending on the inclination angle between the spin and magnetic axes (see eqn. (7) and Figure 5). Disks that start their evolution with the inner radius far inside the light cylinder may evolve to the situation where the inner disk radius reaches the light cylinder. In this case and even further the electromagnetic stresses of the fields generated by the neutron star can balance the material stresses from the disk. Near the light cylinder the power-law index of the electromagnetic energy density γ_L varies between -5.4 (for $\xi = 0^\circ$) and -4.5 (for $\xi = 90^\circ$) (see Eq. (6) and Fig 4). Assuming a thin Shakura-Sunyaev disk with $\mathcal{E}_K \propto r^{-23/8}$ does not change these conclusions qualitatively and a stable inner radius can be found at least up to $\cong 2$ times the light cylinder radius for orthogonal rotators while this critical radius inside which stable equilibrium can be found may extend up to a few ten times the light cylinder for small inclination angles.

When the inner radius of the disk is outside the light cylinder, the pulsar activity is likely to turn on. The presence of the disk may effect the coherent radio emission. The magnetic dipole radiation torque will act on the neutron star even if a radio pulsar is not observed. Sources on their evolutionary path to higher or lower mass inflow rates will make a transition from or to a stage with a disk inner radius stably placed in the radiation zone, and with possible rotation powered activity. Millisecond X-ray pulsars are likely examples of late stages in the evolution of LMXBs into millisecond radio pulsars through spin-up by accretion (Alpar et al. 1982; Radhakrishnan & Srinivasan 1982). Such sources might hover around the transition, exhibiting transient behaviour. The stable presence of the disk outside the light cylinder for a wide range of mass inflow rates makes repeated transitions and sustained transient behaviour possible not only around the transition between propeller and accretion phases, but also around the transition of the inner radius of the disk across the light cylinder.

We thank Ünal Ertan, Rashid Sunyaev and Ed van den Heuvel for discussions. KYE thanks Nihal Ercan for her encouragement. This work was supported by Sabancı University Astrophysics and Space Forum, by the High Energy Astrophysics Working Group of TÜBİTAK (The Scientific and Technical Research Council of Turkey) and by the Turkish Academy of Sciences for MAA.

REFERENCES

- Alpar, M. A. 2001, *ApJ*, 554, 1245.
 Alpar, M. A., Cheng, A.F., Ruderman, M.A. & Shaham, J., 1982, *Nature*, 300, 728
 Alpar, M. A., Ankay, A., and Yazgan, E. 2001, *ApJ*, 557, L61
 Belinski, V., Paolis, F.De, Lee, H.W., & Ruffini, R., 1994, *Å*, 283, 1018
 Blackman, E.G., & Perna, R., 2004, *ApJ*, 601, L71
 Burderi, L., Di Salvo, T, D'Antona, F., Robba, N.R., & Testa, V., 2003, *Å*, 404, L43
 Campana, S. et al. 1998, *ApJ*, 499, L65
 Campana, S. et al. 2002, *ApJ*, 575, L15
 Campana, S. et al. 2002, *ApJ* accepted, astro-ph/0408584
 Chatterjee, P., Hernquist, L., and Narayan, R. 2000, *ApJ*, 534, 373
 Davidson, K., Ostriker, J.P., 1973, *ApJ*, 179, 585
 Davis, L. & Goldstein, M., 1970, *ApJ*, 159, L81.
 Deutsch, A.J., 1955, *Annales D'Astrophysique*, 18, 1.
 Di Salvo, T., Burderi, L., 2003, *Å*397, 723
 Ekşi, K.Y., Alpar, M.A., 2003, *ApJ*, 599, 450.
 Elsner, R.F., Lamb, F.K., 1977, *ApJ*, 215, 897.
 Fabian, A.C., 1975, *MNRAS*, 173, 161
 Frank, King & Raine 2002, *Accretion Power in Astrophysics*, Cambridge University Press
 Goldreich, P., Julian, W.H., 1969, *ApJ*, 157, 869.
 Illarionov, A.F., Sunyaev, R.A., 1975, *Å*, 39, 185.
 Kaburaki, O., 1981, *Ap&SS*, 74, 333.
 Kaspi, V.M., in *IAU Symp.* 218, *Young Neutron Stars and their Environments*, ed. F. Camilo & B.M. Gaensler (San Francisco: ASP), 231
 Lamb, F.K., Pethick, C.J., Pines, D., 1973, *ApJ*, 184, 271
 Li, X.-D., 2002, *ApJ*, 579, L37.
 Lipunov, V.M., 1992, *Astrophysics of Neutron Stars* (Berlin: Springer)
 Marsden, D., Lingener, R.E., Rothschild R.E., & Higdon, J.C., 2001, *ApJ*, 550, 397.
 Marsden, D., Lingener, R.E., & Rothschild R.E., 2001, *ApJ*, 547, L45.

- Marsden, D., Lingenfelter, R.E., & Rothschild R.E., 2002, *Mem. Soc. Astron. Italiana*, 73, 566.
 Melatos, A., 1997, *MNRAS*, 288, 1049.
 Menou, K., Perna R., & Hernquist, L. 2001a, *ApJ*, 554,L63.
 Mereghetti, S., Chiarlone, L., Israel, G.L. & Stella, L., 2002, in *Neutron Stars, Pulsars, and Supernova Remnants*, ed. W. Becker, H. Lesch, & J. Trümper (MPE Rep., 278; Garching: MPE), 29.
 Michel, F.C., 1991, *Theory of Neutron Star Magnetospheres*, University of Chicago Press.
 Michel, F.C., Dessler, A.J., 1981, *ApJ*, 251, 654
 Michel, F.C., & Goldwire, H.C., 1970, *ApJL*, 5, 21.
 Michel, F.C., Li, H., 1999, *Electrodynamics of Neutron Stars*, *Phys. Rep.*, 318, 227.
 Mineshige, S., Nomura, H., Hirose, M., Nomoto, K. & Suzuki, T., 1997, *ApJ*, 489, 227.
 Ostriker, J.P., Gunn, J.E., 1969, *ApJ*, 157, 1395.
 Pacini, F., 1967, *Nature*, 216, 567.
 Pacini, F., 1968, *Nature*, 219, 145.
 Pringle, J.E., Rees, M.J., 1972, *Å*, 21, 1
 Radhakrishnan, V. & Srinivasan, G., 1982, *Curr. Sci.*, 51, 1096
 Shakura, N.I., Sunyaev, R.A., 1973, *Å*, 24, 337
 Shvartsman, V. F., 1970, *Radiofizika* 13:1852
 Shvartsman, V. F., 1970, *Astron. Zh.*, 47, 660
 Treves, A., Szuszkiewics, E., *MNRAS*, 275, 1215
 Wijnands, R., van der Klis, M., 1998, *Nature*, 394, 344
 Wijnands, R., 2004, in "The Restless High Energy Universe", eds. E.P.J. van den Heuvel, J.J. M. in 't Zand, & R.A.M. Wijers (Elsevier)
 Woosley, S.E., Heger, A. & Weaver, T.A., 2002, *Rev. Mod. Phys.*, 74(4),1015.
 Zamanov, R., 1995, *MNRAS*, 272, 308.

APPENDIX

THE DEUTSCH (1955) SOLUTIONS

For an inclination angle ξ , equatorial magnetic field strength B_0 , and stellar radius R_* , the solutions in spherical coordinates (r, θ, ϕ) are the following (Michel & Li (1999), Eqns. 89 & 90):

$$\begin{aligned} B_r &= 2B_0 \frac{R_*^3}{r^3} \{ \cos \xi \cos \theta + \sin \xi \sin \theta [d_1 \cos \psi + d_2 \sin \psi] \}, \\ B_\theta &= B_0 \frac{R_*^3}{r^3} \{ \cos \xi \sin \theta - \sin \xi \cos \theta [(q_1 + d_3) \cos \psi + (q_2 + d_4) \sin \psi] \}, \\ B_\phi &= B_0 \frac{R_*^3}{r^3} \sin \xi \{ - [q_2 \cos 2\theta + d_4] \cos \psi + [q_1 \cos 2\theta + d_3] \sin \psi \} \end{aligned} \quad (\text{A1})$$

and

$$\begin{aligned} E_r &= \frac{E_0}{c} \frac{\alpha^2}{x^2} \left\{ \frac{2}{3} \cos \xi + \frac{\alpha^2}{x^2} \cos \xi (1 - 3 \cos^2 \theta) - \frac{3}{x^2} \sin \xi \sin 2\theta [q_1 \cos \psi + q_2 \sin \psi] \right\}, \\ E_\theta &= \frac{E_0}{c} \frac{\alpha^2}{x^2} \left\{ -\frac{\alpha^2}{x^2} \cos \xi \sin 2\theta + \sin \xi [(q_3 \cos 2\theta - d_1) \cos \psi + (q_4 \cos 2\theta - d_2) \sin \psi] \right\}, \\ E_\phi &= \frac{E_0}{c} \frac{\alpha^2}{x^2} \sin \xi \cos \theta [(q_4 - d_2) \cos \psi - (q_3 - d_1) \sin \psi] \end{aligned} \quad (\text{A2})$$

Here

$$\psi = \phi - \Omega t + x - \alpha \quad (\text{A3})$$

where Ω is the angular velocity of the star,

$$x = \frac{r}{R_L} = \frac{r\Omega}{c} \quad (\text{A4})$$

and

$$\alpha = \frac{R_*}{R_L} = \frac{R_* \Omega}{c} = 6.28 \times 10^{-3} \left(\frac{P}{100ms} \right)^{-1}. \quad (\text{A5})$$

For usual rotation rates $\alpha \ll 1$. Moreover,

$$E_0 = \Omega R_* B_0 = c \alpha B_0 \quad (\text{A6})$$

and the non-constant coefficients are

$$\begin{aligned} d_1 &= \frac{\alpha x + 1}{\alpha^2 + 1}, & d_2 &= \frac{x - \alpha}{\alpha^2 + 1}, \\ d_3 &= \frac{1 + \alpha x - x^2}{\alpha^2 + 1}, & d_4 &= \frac{(x^2 - 1)\alpha + x}{\alpha^2 + 1} \end{aligned} \quad (\text{A7})$$

and

$$q_1 = \frac{3x(6\alpha^3 - \alpha^5) + (3 - x^2)(6\alpha^2 - 3\alpha^4)}{\alpha^6 - 3\alpha^4 + 36}, \quad (\text{A8})$$

$$q_2 = \frac{(3 - x^2)(\alpha^5 - 6\alpha^3) + 3x(6\alpha^2 - 3\alpha^4)}{\alpha^6 - 3\alpha^4 + 36},$$

$$q_3 = \frac{(x^3 - 6x)(\alpha^5 - 6\alpha^3) + (6 - 3x^2)(6\alpha^2 - 3\alpha^4)}{x^2(\alpha^6 - 3\alpha^4 + 36)}, \quad (\text{A9})$$

$$q_4 = \frac{(6 - 3x^2)(\alpha^5 - 6\alpha^3) + (6x - x^3)(6\alpha^2 - 3\alpha^4)}{x^2(\alpha^6 - 3\alpha^4 + 36)}. \quad (\text{A10})$$

We assume the disk to be at the $\theta = \pi/2$ plane where the field components given in (A1) and (A2) simplify to

$$\begin{aligned} B_r &= \frac{2\mu}{R_L^3 x^3} \sin \xi (d_1 \cos \psi + d_2 \sin \psi), \\ B_\theta &= \frac{\mu}{R_L^3 x^3} \cos \xi, \\ B_\phi &= \frac{\mu}{R_L^3 x^3} \sin \xi [(q_2 - d_4) \cos \psi + (d_3 - q_1) \sin \psi] \end{aligned} \quad (\text{A11})$$

where $\mu = B_0 R_*^3$ and using (A6) in (A2)

$$\begin{aligned} E_r &= \frac{\mu}{R_L^3 x^2} \cos \xi \left(\frac{2}{3} + \frac{\alpha^2}{x^2} \right), \\ E_\theta &= -\frac{\mu}{R_L^3 x^2} \sin \xi [(q_3 + d_1) \cos \psi + (q_4 + d_2) \sin \psi], \\ E_\phi &= 0. \end{aligned} \quad (\text{A12})$$

We obtain the radial component of the Poynting vector $\mathbf{S} = (c/4\pi)\mathbf{E} \times \mathbf{B}$ at the disk plane ($\theta = \pi/2$) from equations (A11) and (A12). Averaging $S_r = \mathbf{S} \cdot \hat{\mathbf{r}}$ over a period, we obtain

$$\left\langle \frac{\mathbf{S}_r}{c} \right\rangle = \frac{\mu^2}{8\pi R_L^6} \frac{\sin^2 \xi}{x^5} s(x) \quad (\text{A13})$$

where

$$s(x) = -[(q_3 + d_1)(q_2 - d_4) + (q_4 + d_2)(d_3 - q_1)] \quad (\text{A14})$$

This can be approximated as

$$s(x) \simeq \begin{cases} \frac{3x^5 + 2\alpha^2 x^3 + \alpha^5}{3x^2} & \text{for } x \sim \alpha; \\ x^3 & \text{for } x \gtrsim \text{a few } \alpha. \end{cases} \quad (\text{A15})$$

We average the square of the fields over one stellar period P as $\langle G_i^2 \rangle = (1/P) \int_0^P G_i^2 dt$ where G_i is any component of the electric or magnetic field.

$$\mathcal{E}_m = \frac{\langle B^2 \rangle}{8\pi} \quad (\text{A16})$$

$$= \frac{\mu^2}{8\pi R_L^6} x^{-6} \left(\cos^2 \xi + \frac{1}{2} f_1(x) \sin^2 \xi \right) \quad (\text{A17})$$

where

$$f_1(x) = (q_2 - d_4)^2 + (d_3 - q_1)^2 + 4d_1^2 + 4d_2^2 \quad (\text{A18})$$

In the limit $\alpha \ll 1$, this simplifies as $f_1(x) = x^4 + 3x^2 + 5$ and we obtain

$$\mathcal{E}_m \simeq \frac{\mu^2}{8\pi R_L^6} x^{-6} \left[\cos^2 \xi + \frac{1}{2} (x^4 + 3x^2 + 5) \sin^2 \xi \right] \quad (\text{A19})$$

Similarly the electric energy density is

$$\mathcal{E}_e = \frac{\langle E^2 \rangle}{8\pi} \quad (\text{A20})$$

$$= \frac{\mu^2}{8\pi R_L^6} x^{-4} \left[\cos^2 \xi \left(\frac{2}{3} + \frac{\alpha^2}{x^2} \right)^2 + \frac{1}{2} f_2(x) \sin^2 \xi \right] \quad (\text{A21})$$

where

$$f_2(x) = (q_3 + d_1)^2 + (q_4 + d_2)^2 \quad (\text{A22})$$

and in the limit $\alpha \ll 1$ this simplifies as $f_2(x) = x^2 + 1$ and we obtain

$$\mathcal{E}_e \simeq \frac{\mu^2}{8\pi R_L^6} x^{-4} \left[\frac{4}{9} \cos^2 \xi + \frac{1}{2} (x^2 + 1) \sin^2 \xi \right] \quad (\text{A23})$$